# Reversible Borylene Formation from Ring Opening of Pinacolborane and Other Intermediates Generated from Five-Coordinate Tris-Boryl Complexes: Implications for Catalytic C−H Borylation

Behnaz Ghaffari, Britt A. Vanchura, II, Ghayoor A. Chotana, Richard J. Staples, Daniel Holmes, Robert E. Maleczka, Jr.,* and Milton R. Smith, III*

Department of Chemistry, Michigan State University, 578 South Shaw Lane, East Lansing, Michigan 48824-1322 United States

S *Supporting Information*

ABSTRACT: Catalytic C−H borylation using the five-coordinate tris-boryl complex (dippe)Ir(Bpin)$_3$ (**5a**, dippe = 1,2-bis(diisopropylphosphino)ethane) has been examined using ^{31}P{^{1}H} and ^{1}H NMR spectroscopy. Compound **5a** was shown to react rapidly and reversibly with HBpin to generate a six-coordinate borylene complex, (dippe)Ir(H)-(Bpin)$_2$(BOCMe$_2$CMe$_2$OBpin) (**6**), whose structure was confirmed by X-ray crystallography. Under catalytic conditions, the H$_2$ generated from C−H borylation converted compound **6** to a series of intermediates. The first is tentatively assigned from ^{31}P{^{1}H} and ^{1}H NMR spectra as (dippe)Ir(H$_2$B$_3$pin$_3$) (**7**), which is the product of formal H$_2$ addition to compound **5a**. As catalysis progressed, compound **7** was converted to a new species with the formula (dippe)Ir(H$_3$B$_2$pin$_2$) (**8**), which arose from H$_2$ addition to compound **7** with loss of HBpin. Compound **8** was characterized by ^{31}P{^{1}H} and ^{1}H NMR spectroscopy, and its structure was confirmed by X-ray crystallography, where two molecules with different ligand orientations were found in the unit cell. DFT calculations support the formulation of compound **8** as an Ir^{III} agostic borane complex, (dippe)IrH$_2$(Bpin)(η^2-HBpin). Compound **8** was gradually converted to (dippe)Ir(H$_4$Bpin) (**9**), which was characterized by ^{31}P{^{1}H} and ^{1}H NMR spectroscopy and X-ray crystallography. DFT calculations favor its formulation as an agostic borane complex of Ir^{III} with the formula (dippe)IrH$_3$(η^2-HBpin). Compound **9** reacted further with H$_2$ to afford the dimeric structure [(dippe)IrH$_2$(μ_2-H)]$_2$ (**10**), which was characterized by ^{1}H NMR and X-ray crystallography. Compounds **7**−**10** are in equilibrium when H$_2$ and HBpin are present.
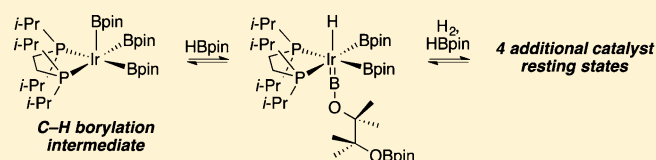
INTRODUCTION

Catalytic C−H borylation is an effective method for preparing organoboron compounds via the dehydrogenative coupling of B−H and C−H bonds.[1] Boryl complexes with the transition metals Ir,[1] Rh,[1] Co,[2−5] Fe,[4−7] and Ni[8] catalyze this process, with a majority of the reported examples utilizing Ir catalysts. Of the Ir catalysts employed, the most commonly invoked intermediates that mediate C−H activation are 16-electron Ir^{III} species of the formula L$_2$Ir(Bpin)$_3$ (**1**, Scheme 1), where L represents a neutral, two-electron-donor ligand that can be monodentate but is more commonly a bidentate ligand such as a bipyridine or bis-phosphine.[9,10]

Experiment and theory support the cycle shown in Scheme 1. C−H activation is rate determining for bipyridine catalysts, where computational studies support an Ir$^{III/V}$ mechanism.[11−13] Phosphine-ligated catalysts have received less attention, although computational studies predict that the intermediates that are generated by C−H activation are Ir^{III}−borane adducts (**2**).[13] Experimental studies for phosphine systems show reduced kinetic isotope effects in comparison to bipyridine-supported catalysts, and the calculated barriers for C−H activation and B−C elimination are similar.[14]

For the widely applied ligand precatalyst combination dtbpy/[Ir(OMe)(cod)]$_2$, rate-limiting C−H cleavage is proposed from

Scheme 1. Catalytic Cycle for C−H Borylation
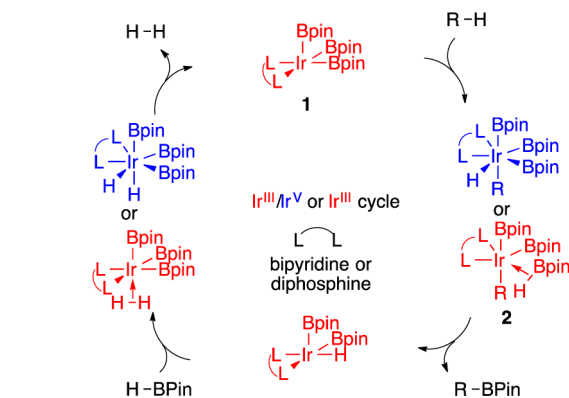
the reaction of the hydrocarbon substrate with the tris-boryl intermediate (dtbpy)Ir(Bpin)$_3$ (**3**). While compound **3** has eluded detection, detailed mechanistic studies of (dtbpy)Ir-

(Bpin)$_3$(coe) (**4**) support its generation from pre-equilibrium dissociation of coe from compound **4**.[9]

Inspired by the stabilization of reactive, low-coordinate complexes with sterically demanding chelating phosphine ligands,[15,16] we targeted 16-electron, 5-coordinate complexes of the general formula (diphosphine)Ir(boryl)$_3$.[17] Indeed, compounds **5a–d** can be prepared by displacing 6e-donor η^6-arenes from arene tris-boryl complexes with 4e-donor diphosphinoethanes, R$_2$PCH$_2$CH$_2$PR$_2$ (Scheme 2, R = *i*-Pr,

Scheme 2. Synthesis of 16-Electron Tris-Boryl Compounds

	R	boryl
5a	*i*-Pr	Bpin
5b	*i*-Pr	Bcat
5c	*t*-Bu	Bpin
5d	*t*-Bu	Bcat
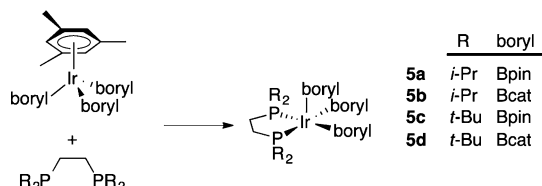
dippe; *t*-Bu, dtbpe).[17−19] The relative reactivity of these complexes is a function of both the steric features of the diphosphine, with relative reactivities dippe ≈ dcpe > dtbpe and the nature of the boryl ligand Bpin ≫ Bcat.[17] These are rare examples where catalytically active intermediates are isolable, enabling the direct examination of fundamental steps in the catalytic cycle. For example, compound **5a** reacts with C(sp^2)−H bonds at room temperature to generate stoichiometric quantities of borylated products.[17]

This room-temperature reactivity is in contrast to catalytic borylations with catalysts generated in situ from Ir precatalysts and chelating phosphines, which require considerably higher temperatures for catalytic turnover. In this paper, a closer inspection of the chemistry of compound **5a** under catalytic conditions shows that it is converted to more stable resting states whose concentrations change during the reaction. This accounts for the decreased catalytic activity in comparison to the relatively facile stoichiometric borylations mediated by compound **5a**.

■ RESULTS

When excess HBpin is added to pale yellow solutions of compound **5a**, a colorless solution results immediately, and ^{31}P{^{1}H} NMR spectroscopy indicates disappearance of the resonance for compound **5a** (δ 86.35) and formation of a new species, compound **6** (δ 67.24). When a 1,3-bis-(trifluoromethyl)benzene solution containing compound **6** and 10 equiv of HBpin was cooled to −35 °C, colorless crystals formed. An X-ray crystallographic analysis revealed the molecular structure of compound **6**. As shown in Figure 1, compound **6** is a borylene diboryl hydride that arises from ring opening of HBpin, which also serves as the hydride source. This is the first complex to have boryl and borylene ligands in the metal coordination sphere.

Metrical data indicate sp hybridization of the borylene boron. The Ir−B distance (1.955(8) Å) is shorter than those for the boryl ligands (2.143(14) and 2.095(8) Å) and is consistent with values for other reported borylenes. ^{11}B NMR spectra show three distinct resonances for compound **6**. The highest field resonance at δ 22.0 is assigned to the OBpin moiety. A downfield resonance at δ 38.8 integrates as two B atoms and has a chemical shift that is typical for Ir boryl ligands. The borylene B is assigned to a broad downfield resonance at δ 54.5. Borylene resonances typically appear at lower field in
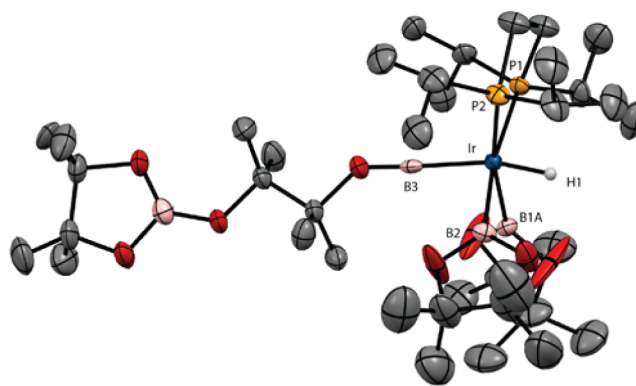

Figure 1. X-ray structure for compound **6** with thermal ellipsoids calculated at 50% probability levels. Disorder in one of the boryl ligands (B1B) and all hydrogens except for the hydride ligand are omitted for clarity.

comparison to those for boryl ligands, though the borylene resonance in compound **6** appears at higher field than is typical for borylenes.[20]

The hydride ligand in compound **6** occupies a position trans to the borylene. The short Ir−H (1.39(5) Å) distance is likely underestimated. A calculated structure of the dmpe analogue (see Table S5 and Figure S12 in the Supporting Information) reproduces distance and angles for the heavy atoms with good fidelity. The calculated B−Ir−H angle (159°) is similar to the experimentally determined value (165(2)°), but the calculated Ir−H distance of 1.70 Å is closer to a typical Ir−H distance determined from neutron diffraction.[21] The hydride ligand's presence is confirmed by a high-field triplet a δ −11.05 ($|^2J_{PH}|$ = 19 Hz) in the ^{1}H NMR spectrum. The magnitude of the P−H coupling and the relatively narrow line widths for the resonance support its formulation as a classical hydride having no interactions with the *cis*-boryl ligands.

A number of borylene complexes have been reported.[20,22] These have been prepared by various synthetic routes, with the H$_2$ elimination/B−H activation described by Sabo-Etienne and co-workers bearing some similarity to the generation of compound **6** in that borylene formation is reversible and arises from B−H activation.[23]

When crystals of compound **6** were dissolved in benzene-d_6, NMR spectra showed resonances for compound **5a** and HBpin, in addition to those for compound **6**. This suggests that compound **6** is in equilibrium with compound **5a** and HBpin. This was confirmed by the diminution of the resonances for compound **5a** when HBpin is added to the solution and the fact that under high vacuum compound **6** reverts to compound **5a**, which prevented us from obtaining consistent elemental analysis for compound **6**. The equilibrium constant for eq 1 is $K_{eq} = 1.65 \times 10^{-3}$ M^{-1}.

$$K_{eq} = 1.65 \times 10^{-3} \text{ M}^{-1} \quad (1)$$

6   **5a**, R = *i*-Pr + HBpin
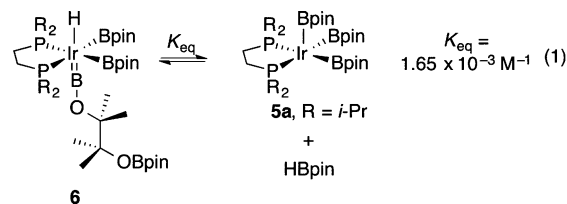
When compound **5a** is used in catalytic quantities for borylation of 2-methylthiophene with HBpin, ^{31}P{^{1}H} NMR spectroscopy shows that the equilibrium in eq 1 is shifted to the
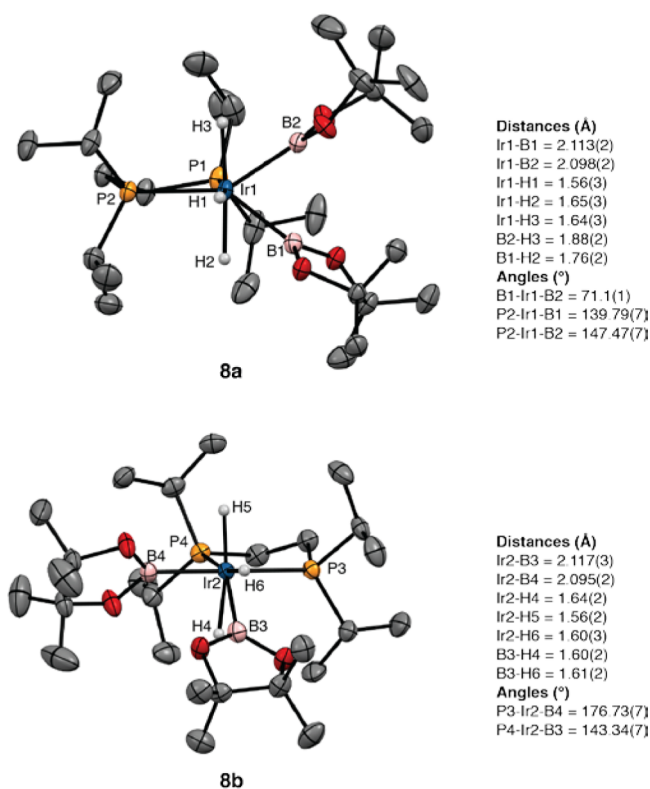
extent that compound **7** is the major species at the beginning of the reaction. If compound **5a** is responsible for borylation, HBpin would inhibit catalysis. This is indeed the case, as *catalytic* borylation of 2-methylthiophene does not proceed at room temperature, despite the fact that $t_{1/2}$ for stoichiometric borylation by compound **5a** at similar concentrations is less than 5 min.[17]

When cyclohexane-d_{12} solutions of compound **5a** (42 mM), HBpin (420 or 840 mM), and 2-methylthiophene (840 mM) are heated, catalytic borylation commences. $^{31}P\{^1H\}$ NMR spectra of the catalytic reaction at 100 °C indicate that, in addition to compound **6**, resonances for other species appear during the reaction at δ 53.42, 61.22, 66.75, and 77.78. At 100 °C, these resonances are sharp. The relative concentrations of these intermediates vary depending on reaction times and ratios of HBpin to thiophene substrate.

After heating at 100 °C for 5 min, the intensity of the resonance for compound **6** in the $^{31}P\{^1H\}$ NMR spectrum decreases and a new feature appears at δ 53.42. This is accompanied by the appearance of a new high-field triplet in the ^1H NMR spectrum at δ −11.16 ($|J_{PH}|$ = 12 Hz). By comparison of intensities for compound **6** and this new feature in the $^{31}P\{^1H\}$ NMR spectrum, the relative integrations of the hydride resonances in the ^1H NMR spectrum indicated that this new peak contributes two hydrides per dippe ligand. The line width of this resonance (9.5 Hz, fwhm) is consistent with B−H coupling, which is higher than that in **6**. We tentatively assign this to a complex with the formula (dippe)Ir(H$_2$B$_3$pin$_3$) (**7**). Consistent with this formulation, compound **7** can be generated independently by adding H$_2$ to compound **5a** (vide infra).

After 10 min of heating, the resonances for compound **6** disappear. The ^{11}B NMR spectrum shows a boryl resonance at δ 37.7 and no low-field resonance for a borylene ligand. At this point another resonance appears in the $^{31}P\{^1H\}$ NMR spectrum at δ 61.22, in addition to the resonance for compound **7**. This is assigned to the complex (dippe)Ir-(H$_3$B$_2$pin$_2$) (**8**). The hydride region in the ^1H NMR spectrum for compound **8** showed a major resonance at δ −11.21 as a broad triplet ($|J_{PH}|$ = 6 Hz). When compound **8** is generated from H$_2$ addition to compound **5a** (vide infra), this resonance integrates as three protons. While we were not able to isolate compound **8** in analytically pure form, single crystals were obtained by cooling solutions of compound **5a** with a 10-fold excess of HBpin. The structure is depicted in Figure 2. Two independent molecules appear in the unit cell, and these differ in the relative orientation of the boryl ligands. In independent molecule **8a**, the boryl ligands are both cis to one of the phosphines, with the P−Ir vector of the other phosphorus approximately bisecting the B1−Ir1−B2 angle. In the second independent molecule (**8b**), one boryl (B4) is trans to P3 and cis to P4, while the second boryl (B3) is cis to P3 and forms a P4−Ir2−B3 angle of 143.34(7)°. The Ir−B distances range from 2.095(2) to 2.117(3) Å and are slightly longer than the Ir−B bonds trans to phosphines in compound **5a** (2.07(1) Å). Electron density was located in regions consistent with hydride ligands and refined, but the difficulty in locating hydrides bound to Ir prevents definitive characterization of H···B interactions, which contribute to the line width of the hydride resonance and the reduced magnitude of $|^1J_{PH}|$.

We turned to theory to gain further insight into the H$_3$B$_2$pin$_2$ framework. Structures were optimized at an M06//SDD/6-31G* level of theory using the X-ray coordinates as a starting

8a

Distances (Å)
Ir1−B1 = 2.113(2)
Ir1−B2 = 2.098(2)
Ir1−H1 = 1.56(3)
Ir1−H2 = 1.65(3)
Ir1−H3 = 1.64(3)
B2−H3 = 1.88(2)
B1−H2 = 1.76(2)
Angles (°)
B1−Ir1−B2 = 71.1(1)
P2−Ir1−B1 = 139.79(7)
P2−Ir1−B2 = 147.47(7)

8b

Distances (Å)
Ir2−B3 = 2.117(3)
Ir2−B4 = 2.095(2)
Ir2−H4 = 1.64(2)
Ir2−H5 = 1.56(2)
Ir2−H6 = 1.60(3)
B3−H4 = 1.60(2)
B3−H6 = 1.61(2)
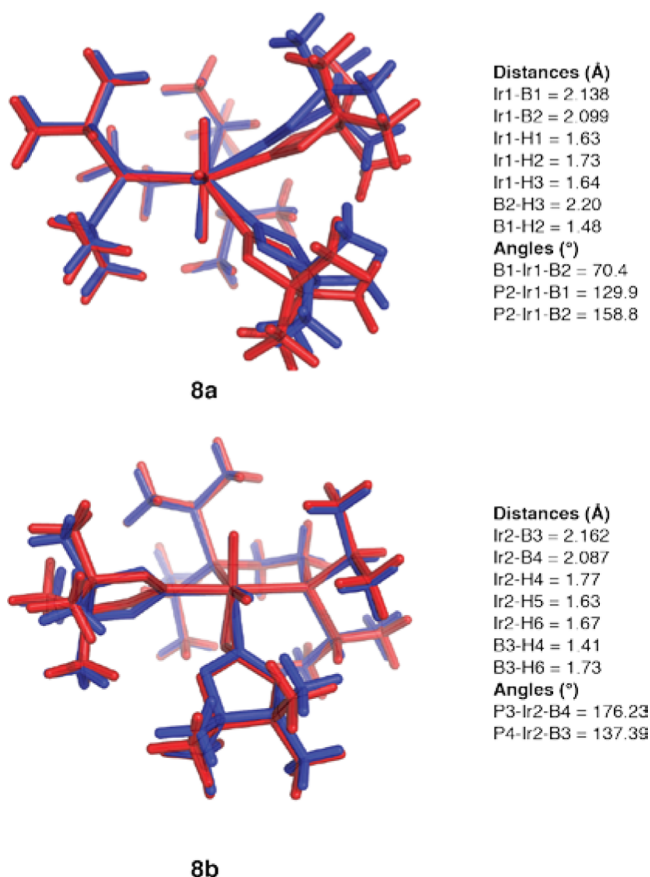Angles (°)
P3−Ir2−B4 = 176.73(7)
P4−Ir2−B3 = 143.34(7)

Figure 2. X-ray structure for compound **8** with thermal ellipsoids calculated at 50% probability levels. The two independent molecules (**8a,b**) are shown with selected angles and distances.

point. Figure 3 shows an overlay of the calculated structures (red) with the coordinates from the X-ray structures (blue). Isomer **8a** is calculated to be 1.5 kcal more stable than isomer **8b**. As can be seen in Figure 3, the calculated coordinates for **8a** are shifted significantly from the experimentally determined values. Essentially, B1 and B2 swing toward H2, leaving the B1−Ir1−B2 angle unchanged. The shift in the calculated structure allows for a significant B···H interaction (1.48 Å) between B1 and H2 and eliminates any interaction between B2 and H3. The structure is best described as an agostic borane complex of an Ir^{III} dihydrido boryl complex, (dippe)-IrH$_2$(Bpin)(η^2-HBpin). For structure **8b**, the calculated structure more closely resembles the experimentally determined one. The biggest changes are a lengthening of the Ir2−B3 distance and a shortening of the B3−H4 distance. As for **8a**, the calculated structure of **8b** is best represented as an Ir^{III} dihydrido boryl complex with one boryl and one agostic HBpin ligand.

With continued heating of the cyclohexane-d_{12} solution, the resonance for compound **7** in the $^{31}P\{^1H\}$ NMR spectrum vanishes and a new resonance at δ 66.75 accompanies the resonance for compound **8**. In the hydride region of the ^1H NMR spectrum, a new resonance also appears as a triplet at δ −11.90 ($|J_{PH}|$ = 17 Hz). When the ^{31}P NMR spectrum is recorded with selective decoupling of the aliphatic protons, the hydride coupling is preserved, and the resulting quintet proves that four hydrides are bound to Ir. This compound was crystallized by cooling a 1,3-bis(trifluoromethyl)benzene solution containing compounds **6**, **8**, and a 10-fold excess of HBpin to −30 °C. After several weeks crystals formed and X-ray diffraction revealed their structure to be (dippe)Ir(H$_4$Bpin) (**9**; Figure 4). Compound **9** could be generated independently

8a

Distances (Å)
Ir1-B1 = 2.138
Ir1-B2 = 2.099
Ir1-H1 = 1.63
Ir1-H2 = 1.73
Ir1-H3 = 1.64
B2-H3 = 2.20
B1-H2 = 1.48
Angles (°)
B1-Ir1-B2 = 70.4
P2-Ir1-B1 = 129.9
P2-Ir1-B2 = 158.8

8b

Distances (Å)
Ir2-B3 = 2.162
Ir2-B4 = 2.087
Ir2-H4 = 1.77
Ir2-H5 = 1.63
Ir2-H6 = 1.67
B3-H4 = 1.41
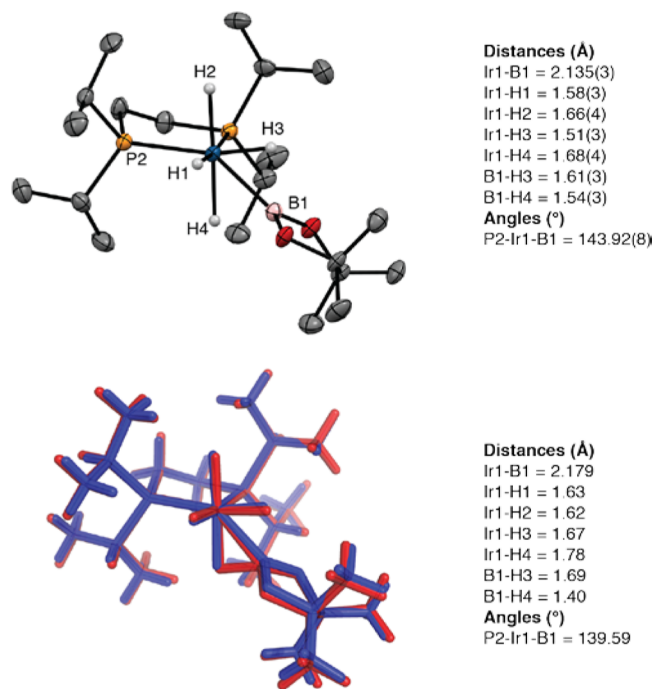B3-H6 = 1.73
Angles (°)
P3-Ir2-B4 = 176.23
P4-Ir2-B3 = 137.39

Figure 3. Calculated structures (M06//SDD/6-31G*) for **8a,b** (red) overlaid with coordinates from their X-ray structures (blue). Calculated bond distances and angles correspond to the numbering scheme in Figure 2.

Distances (Å)
Ir1-B1 = 2.135(3)
Ir1-H1 = 1.58(3)
Ir1-H2 = 1.66(4)
Ir1-H3 = 1.51(3)
Ir1-H4 = 1.68(4)
B1-H3 = 1.61(3)
B1-H4 = 1.54(3)
Angles (°)
P2-Ir1-B1 = 143.92(8)

Distances (Å)
Ir1-B1 = 2.179
Ir1-H1 = 1.63
Ir1-H2 = 1.62
Ir1-H3 = 1.67
Ir1-H4 = 1.78
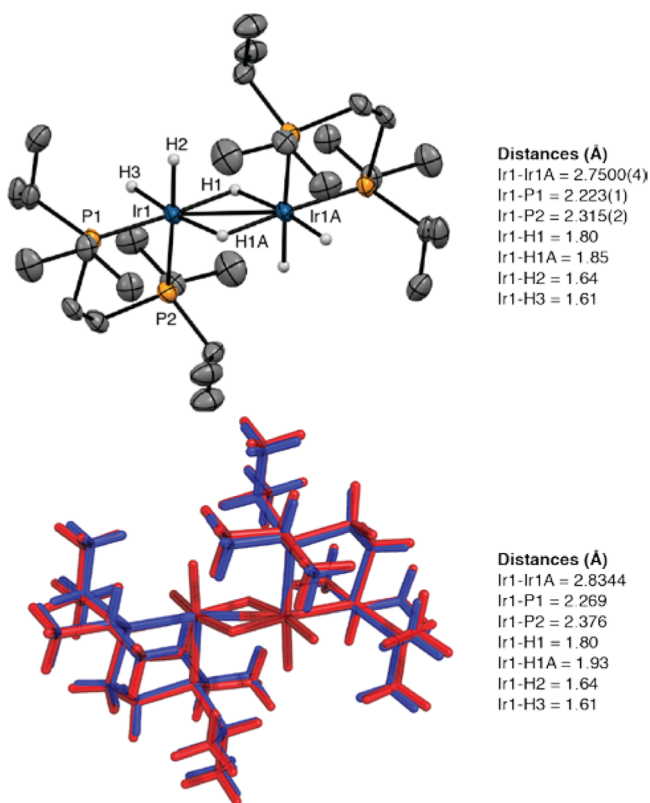B1-H3 = 1.69
B1-H4 = 1.40
Angles (°)
P2-Ir1-B1 = 139.59

Figure 4. X-ray structure for compound **9** with thermal ellipsoids calculated at 50% probability levels. Hydride ligands are shown, and other hydrogens are omitted for clarity. The calculated structure (red, M06//SDD/6-31G*) is overlaid with crystallographic coordinates. Selected experimental and computational metric parameters are given.

by exposing a THF solution of compound **5a** in a Schlenk flask to excess H_2 for 30 min. $^{31}P\{^1H\}$ NMR spectra of the crude mixture indicated the presence of compounds **9** (80%), **8** (5%), and other unidentified species.

The crystal structure of compound **9** is shown in Figure 4. Hydrides were located and refined, but the usual caveat applies to the certainty of their positions. The Ir1−B1 distance is relatively long in comparison to the other boryl ligands in this family of complexes and may reflect contributions from agostic borane or borohydride structures. We carried out calculations starting from the X-ray coordinates, and the calculated structure (red) is shown with its overlap to the crystallographic coordinates (blue). There is good agreement between the calculated and experimental structure, with the biggest differences being elongation of the Ir1−B1 bond and B1−H3 distance with a shortening of the B1−H4 distance in the calculated structure, which is best described as a borane adduct of an Ir^{III} trihydride. On the basis of the ^1H and $^{31}P\{^1H\}$ NMR data, the hydride positions are rapidly equilibrating on the NMR time scale.

With continued heating of the catalytic reaction, the resonance for compound **9** loses intensity, accompanied by the appearance of a new resonance at δ 77.78 in the $^{31}P\{^1H\}$ NMR spectrum. The intensity of this resonance is a maximum at the end of reactions where the initial [HBpin]:[thiophene] = 0.5. When a cyclohexane-d_{12} solution is cooled to 5 °C, the $^{31}P\{^1H\}$ resonance resolves into four distinct features at δ 78.77, 78.07, 76.52, and 76.16. These features are slightly

temperature and solvent dependent, as the $^{31}P\{^1H\}$ NMR spectrum in toluene-d_8 solution at −68 °C has peaks at δ 77.46, 76.88, 75.79, and 74.96. ^1H NMR spectra at 500 MHz and 5 °C in cyclohexane-d_{12} show a complex pattern in the hydride region with resonances clustered at δ −3.77, −13.23, and −22.55. The three resonances have equal integrations, and a ^1H COSY spectrum indicates that they are all coupled. At 70 °C the two lower-field hydrides vanish and a broad high-field resonance is observed at δ −22.73.

X-ray-quality crystals were obtained by dissolving the crude reaction mixture in pentane and cooling to −35 °C. The X-ray crystal structure in Figure 5 reveals the dimeric structure **10**, where each Ir center is κ^2 bound to a dippe ligand. The hydride ligands could not be located. The structure was refined with the constraints of one bridging and two terminal hydrides for each Ir center using distances from the calculated structures. The bridging hydride was fixed with the shorter Ir−H distance. The metrical parameters for all other atoms in constrained and unconstrained refinements were identical within error limits. The hydride formulation is consistent with the hydride resonances in the high-temperature NMR spectra (vide infra). Calculations starting from the X-ray coordinates refine to a similar structure with a slight elongation of the Ir−Ir distance. Attempts to calculate the structure as [(dippe)IrH(μ-H)]$_2$ with one terminal and one bridging hydride gave geometries where the non-hydrogen atoms were shifted significantly from the crystallographically determined positions (see the Supporting Information for details).

The relationship among compounds **5a** and **7−10** was established by independent NMR experiments. When H_2 was admitted to an NMR tube containing a toluene-d_8 solution of compound **5a**, $^{31}P\{^1H\}$ and ^1H NMR spectra at −45 °C showed that compound **7** is the major species in solution along

Distances (Å)
Ir1–Ir1A = 2.7500(4)
Ir1–P1 = 2.223(1)
Ir1–P2 = 2.315(2)
Ir1–H1 = 1.80
Ir1–H1A = 1.85
Ir1–H2 = 1.64
Ir1–H3 = 1.61

Distances (Å)
Ir1–Ir1A = 2.8344
Ir1–P1 = 2.269
Ir1–P2 = 2.376
Ir1–H1 = 1.80
Ir1–H1A = 1.93
Ir1–H2 = 1.64
Ir1–H3 = 1.61

Figure 5. X-ray structure for compound **10** with thermal ellipsoids calculated at 50% probability levels. Hydride ligands are shown, and other hydrogens are omitted for clarity. The calculated structure (red, M06//SDD/6-31G*) is overlaid with crystallographic coordinates (blue). Selected experimental and computational metric parameters are given.

since compound **5a** is generated from compound **6** by its dissociation. This is not observed experimentally, as the H_2 generated (observed in the ^{1}H NMR spectra) during C−H borylation sequentially shifts the resting state to 18-electron compounds **7**−**9**. Thus, these complexes are more stable than borylene compound **6**.

^{1}H NMR spectroscopy yields important information about the 18-electron catalytic resting states **7**−**9**. Significantly, the inequivalent hydride/borane/boryl positions indicated in the solid-state structures of compounds **8** and **9** are exchanging rapidly on the NMR time in solution. In addition, a single methine resonance for the dippe isopropyl groups is observed, even though the crystal structures in Figures 2 and 4 feature chemically distinct methine environments. These exchanges are intramolecular, since coupling to ^{31}P is maintained and exchange with free HBpin is not observed. The dynamic behavior suggests that minima in the potential energy surface are relatively shallow, which is supported by the fact that compound **8** crystallizes with structures where the orientations of the ligands differ significantly. Scheme 3 shows a pathway

Scheme 3. Putative Equilibria for Hydride Exchange in Compound 8

with compound **8**. ^{31}P NMR spectra with selective decoupling of the aliphatic ^{1}H region gave a broad triplet at δ 53.56, which confirms that two high-field H atoms are chemically equivalent on the NMR time scale in compound **7**. When the NMR tube was removed from the spectrometer and shaken to dissolve H_2 in the headspace, compound **8** became the dominant species in solution. When this process was repeated, compound **8** was converted to compound **9**. Compounds **7**−**9** give single, distinct resonances for each species at −45 °C, indicating that exchange is still fast on the NMR time scale. Finally, equilibration of compounds **8** and **9** with compound **10** was demonstrated by removing the H_2 from an NMR tube where catalytic borylation was complete, leaving compound **10** as the major species. Addition of HBpin to the solution regenerated compounds **8** and **9**.
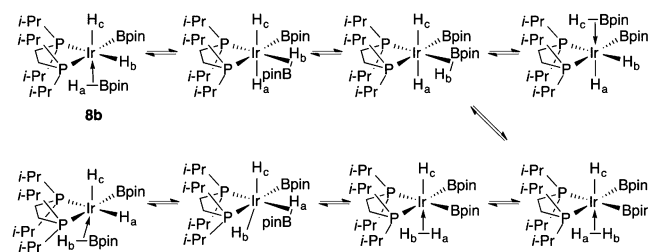
■ DISCUSSION

Compound **5a** joins a handful of complexes that react directly with C−H bonds without requiring prior ligand dissociation[24,25] and is a rare example of a square-pyramidal 16-electron d[6] complex.[26] In accord with the tenet that true reactive intermediates are rarely observed under catalytic conditions,[27] compound **5a** reacts with HBpin to form a more stable initial resting state in 18-electron borylene compound **6**, and compound **5a** is not detected as an intermediate during catalysis. If compound **6** were the only resting state during catalysis and compound **5a** were the only C−H activating intermediate, C−H borylation would be inhibited by HBpin,

where equilibration of σ-HBpin and σ-H_2 intermediates would exchange the hydride ligands in structure **8b**. Similar mechanisms have been proposed to account for exchange in (κ^3-C$_6$H$_3$-1,3-[OP(tBu)$_2$]$_2$)IrH$_2$(η^2-HBpin).[21,28] Calculations support σ-borane complexation in compounds **8** and **9**, which would account for the broadening of high-field resonances in the ^{1}H NMR spectra of these compounds.

Compound **10** is related to other Ir phosphine complexes with bridging hydrides. The most relevant compound is [(dfepe)Ir(μ-H)(H)$_2$]$_2$ (**11**; dfepe = (C$_2$F$_5$)$_2$PCH$_2$CH$_2$P-(C$_2$F$_5$)$_2$).[29] The [(diphosphine)Ir]$_2$ frameworks of compounds **10** and **11** are very similar, although the latter compound is disordered in the solid state. As in compound **11**, the Ir−P distance in **10** for the phosphorus trans to the terminal hydride (2.315(2) Å) is significantly longer than the distance for the phosphorus trans to the bridging hydride (2.223(1) Å). This is consistent with the strong trans influence for terminal hydrides.

In contrast, the spectroscopic features for compound **10** differ from those for compound **11**. Both ^{1}H and ^{31}P{^{1}H} NMR spectra (toluene-d_8 solutions) for compound **10** are more complicated than would be expected for a static structure analogous to that in Figure 5. At 25 °C, the resonances in the hydride and methine regions for compound **10** are relatively broad, suggesting dynamic behavior for compound **10**. At lower temperatures, the hydride resonances sharpen, and at −68 °C, the methine resonance begins to decoalesce with two broad peaks near δ 3.6. At higher temperature the methine peaks coalesce to a broad resonance at δ 2.5. This implies that a second set of methine resonances should appear near δ 1.4 in

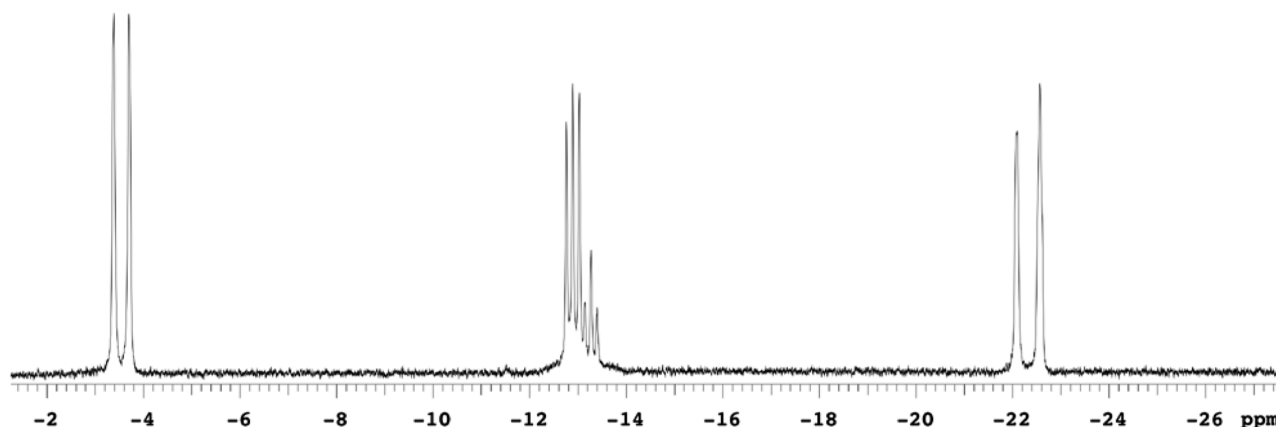**Figure 6.** ^{1}H NMR spectrum (500 MHz, toluene-d_8, −5 °C) of the hydride region for compound **10**.

the low-ttemperature spectrum, where four methine resonances would be expected for the structure in Figure 5, but these are obscured by other features. At low temperature, the hydride region (Figure 6) is complex—particularly for the feature at δ ∼−13. We originally questioned whether a trace impurity gives rise to the triplet at δ −13.06, but this feature persisted when compound **10** was prepared independently from compound **9**, generated in situ from compound **5a** and H$_2$, and 3 equiv of MeOH. At low temperature, the ^{31}P NMR spectrum for compound **10** has four absorptions between δ 78.72 and 76.15 for the phosphorus nuclei, whereas compound **11** has a singlet at δ 84.3. The phosphorus atoms in the crystal structure of compound **10** (Figure 5) are clearly chemically inequivalent. Therefore, P−P coupling would be expected. Because the chemical shift differences have energies similar to the expected coupling, we considered whether the ^{31}P{^{1}H} and ^{1}H NMR spectra reflected second-order coupling. However, the spectra could not be successfully simulated. The ^{1}H COSY spectrum for compound **10** indicates coupling between the features at δ −3.33, −13.00, and −22.12, but selective decoupling of specific hydride resonances did not simplify the other hydride resonances. Thus, H−H couplings are small. Selective ^{31}P decoupling showed that the resonance at δ −3.33 is a doublet ($|^2J_{PH}|$ = 166 Hz). A large coupling would be expected for terminal hydride H2 in Figure 5, since it is trans to P2. In contrast, the apparent doublet centered at δ −22.12 did not collapse when the ^{31}P resonances were irradiated, indicating that the two resonances at δ −21.83 and −22.40 represent two hydride environments. This is consistent with the observed spectra arising from two conformations with similar populations and the same formula as compound **10**. From chemical shifts, we assign the resonances for compound **10** at δ −3.33 and −13.00 to terminal hydrides and the resonances at δ −21.83 and −22.40 to bridging hydrides. This assignment is based on compound **11**, where the terminal hydrides appear as a doublet at δ −7.09 ($|^2J_{PH}|$ = 149 Hz)—the approximate average chemical shift of the two lower field hydride resonances in compound **10**—and the bridging hydrides are assigned to a resonance at δ −21.90.

When the temperature is raised, the hydride resonances in the ^{1}H NMR spectrum broaden, and at 70 °C the resonances clustered at δ −3.33 and −13.00 vanish, which would be consistent with exchange between these hydrides, as is the case for compound **11**. In addition, the ^{31}P resonances coalesce to a single resonance at δ 76.68. This supports exchange between the conformations observed at lower temperatures. Coales-

cence of the lower field hydride resonances was not observed, because compound **10** converts to a new species at higher temperatures. This is indicated by a new major ^{31}P NMR peak at δ 87.91 and ^{1}H NMR peaks at δ −6.80 (dd), −12.33 (br), and −13.01 (br), which integrate as 2:1:2. While it is tempting to assign this as a pentahydride structure of the formula (dippe)IrH$_5$, it is unclear what the sources of H$_2$ would be, and there is a broad feature in the ^{31}P NMR spectrum at δ ∼63 that we cannot assign. We have insufficient data to definitively assign a structure for this species.

Of the intermediates observed in the catalytic reaction, the ligation of H and Bpin ligands in compound **7** can only be tentatively assigned without a crystal structure. Forms **7a**−**c** are possible (Chart 1). Access to structures **7a,b** would lead to B−

Chart 1
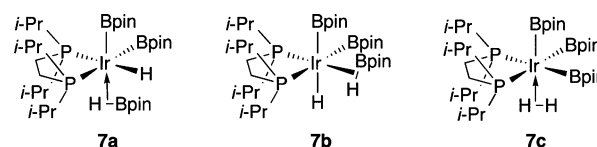
H coupling, which would account for the relatively broad hydride resonance for compound **7**. Equilibration with structure **7c** allows for exchange if **7a,b** are minimum energy structures. If **7c** is the lowest energy structure, the equivalence of the H positions is directly accounted for. Access to structure **7c** could also be relevant to catalysis (Scheme 1), as H$_2$ dissociation would generate C−H borylation intermediate **5a**.

The shift in catalyst resting structures can be understood in terms of equilibria of boryl complexes and H$_2$, whose concentration increases throughout the reaction. As shown in Scheme 4, H$_2$ equilibration with boryl complexes generates HBpin and hydride intermediates with successive substitution of H for Bpin at the Ir center.

If C−H borylation funnels exclusively through intermediate **5a**, H$_2$ generation would significantly inhibit catalysis. This is not the case, as borylation proceeds smoothly until compound **10** is the dominant solution species. Maintenance of borylation activity while compounds **7**−**9** have significant concentrations can be reconciled if these species are resting states for catalytically competent tris (**5a**)-, bis (**12**)-, and mono-boryl (**13**) intermediates that operate in parallel catalytic borylation cycles, with similar borylation rates, as shown in Scheme 5. This behavior is reminiscent of the stoichiometric reactivity of

Scheme 4. H₂-Induced Equilibria by H₂ Addition to Compound 5a
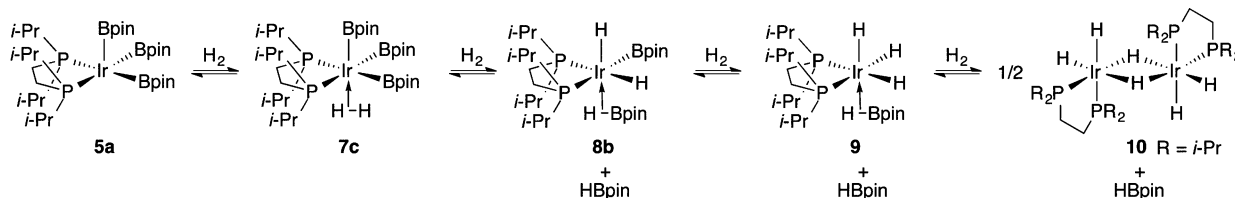
Scheme 5. Parallel Catalytic Cycles for C−H Borylation
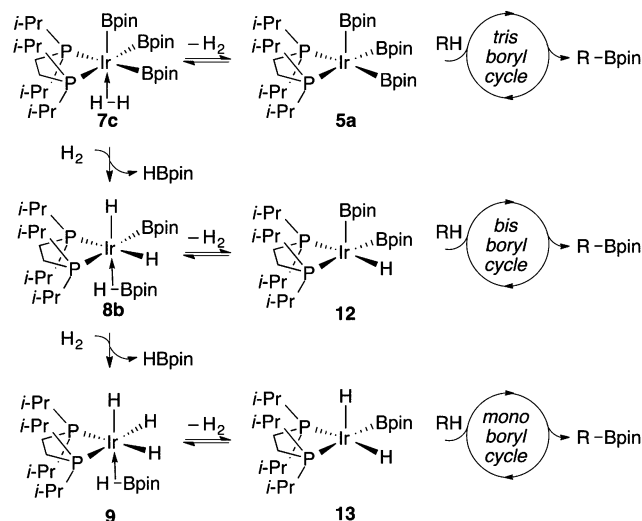
bipyridine-ligated compound **3**, which reacts to generate diboryl hydride and monoboryl dihydride complexes in reactions with arenes.[9] Potential roles for these complexes in catalysis were not examined, and trihydride complexes were not reported.

■ CONCLUSIONS

The fact that compound **5a** reacts directly with C(sp²)−H bonds provides a rare opportunity for examining the fundamental step in C−H borylation. The combination of ³¹P and ¹H NMR spectroscopy, X-ray crystallography, and theory makes it possible to characterize multiple resting states and to assess their roles under catalytically relevant conditions. Although catalysts with bidentate nitrogen donors have been used more extensively, the recent chemistry of phosphine-ligated catalysts suggests that they have as yet unrealized potential.[30,31] The work described herein provides a foundation for understanding catalysis in this family of compounds, which may aid in designing new borylation catalysts.

■ EXPERIMENTAL SECTION

General Procedures. All commercially available chemicals were used as received unless otherwise indicated. Pinacolborane (HBpin containing 1% NEt₃) was generously supplied by BoroPharm, Inc. (η^6-mesitylene)Ir(Bpin)₃ and compound **5a** were prepared by the literature procedures.[17] Solvents were refluxed over sodium benzophenone ketyl, distilled, and degassed. All experiments were carried out in a glovebox under a nitrogen atmosphere or with standard Schlenk techniques.

Analytical Methods. ¹H NMR spectra were recorded on a Varian VXR-500 or Varian Unity-500-Plus spectrometer (499.74 MHz) and referenced to residual solvent signals. ¹¹B NMR spectra were recorded on a Varian VXR-500 spectrometer operating at 160.41 MHz. ³¹P NMR spectra were recorded on a Varian Unity-500-Plus spectrometer

operating at 202.29 MHz. ¹¹B and ³¹P NMR spectra were indirectly referenced relative to SiMe₄ according to the IUPAC standard using VnmrJ software. All coupling constants are apparent J values measured at the indicated field strengths. Melting points were measured on a MEL-TEMP or Thomas-Hoover capillary melting apparatus and are uncorrected.

Note: because all of the compounds are in equilibrium with each other, it was not possible to isolate bulk samples containing one species for combustion analysis.

X-ray Crystallography Details. Crystal structures of compounds **6** and **8**−**10** were determined using a Bruker CCD X-ray diffractometer and associated software, applying standard crystallographic techniques. Specifics for compound **6** include a disorder model for one boryl group, modeled at a 50:50 population. No restraints or constraints were performed to keep the groups together, although the thermal parameters were large for oxygen atoms on one of the boryls. Compounds **8** and **9** were solved without incident, and the hydride atoms were found and refined isotropically. Compound **10** was solved without a problem, but the hydride atoms on the Ir atom could not be located. These were then modeled as riding atoms on the basis of calculated positions generated in theoretical calculations (red, M06// SDD/6-31G*).

Computational Methods. DFT quantum chemical calculations were carried out using the Gaussian 09 software suite (Revision D.01)[32] using the M06 functional.[33] A split basis set was employed with an SDD basis and core potential on Ir and a 6-31G* basis set on the other atoms. Structures were minimized until program default convergence limits were reached.

Synthesis of (dippe)IrH(Bpin)₂(═BOCMe₂CMe₂OBpin) (6). HBpin (8.7 μL, 0.06 mmol, 1 equiv) was added to a pentane solution (1.0 mL) of compound **5a** (50 mg, 0.06 mmol, 1 equiv) in a 20 mL scintillation vial. The initially yellow solution lightened upon addition of the HBpin. The resulting solution was stirred for approximately 2 min when a white precipitate began forming. The vial was placed in a freezer at −35 °C and allowed to sit overnight. The next day the mother liquor was pipetted from the vial, leaving a white solid on the sides of the vial. Nitrogen was blown from a pipet to dry the white solid (43 mg, 75%, mp 151−153 °C).

When the solid was placed back into solution for NMR characterization, the yellow color of the initial reaction solution reappeared. ¹H NMR (benzene-d_6, 500 MHz): δ 2.37−2.30 (m, 2 H), 1.97 (s, 6 H), 1.80−1.72 (m, 2 H), 1.68 (s, 6 H), 1.29 (s, 28 H), 1.19−1.12 (m, 6 H), 1.12−1.06 (m, 6 H), 1.06−1.00 (m, 18 H, boryl singlet 1.05 ppm), 0.94−0.89 (m, 6 H), −11.05 (t, J = 19.3 Hz). ¹¹B NMR (benzene-d_6, 160 MHz): δ 22.0, 38.8, 54.5. ³¹P NMR (benzene-d_6, 202 MHz): δ 67.24.

Calculation of the Equilibrium Constant among Compound 5a, HBpin, and Compound 6. A 0.01 mmol portion of compound **6** was weighed in a test tube and then transferred to a J. Young tube after dissolution in benzene-d_6 (500 μL). When the ³¹P{¹H} and ¹H NMR spectra were recorded, peaks for compounds **6** (67.24 ppm) and **5a** (86.35 ppm) were observed in a roughly 3:1 ratio. The equilibrium constant was calculated from molar ratios determined by integrating resonances in the ¹H NMR spectrum for the HBpin hydride and the methine protons in compounds **5a** and **6** (compound **6** has two sets of methine peaks), which gave K_{eq} = 0.00165 mol L⁻¹. See Figures S1, S2a, and S2b in the Supporting Information.

Catalytic Borylation of 2-Methylthiophene with Compound 5a, using 0.5 equiv of HBpin. Compound **5a** (20.8 mg, 0.025 mmol, 0.05 equiv) was weighed in a test tube and then transferred to a

J. Young NMR tube after dissolution in cyclohexane-d_{12} (150 μL × 4). 2-Methylthiophene (49 μL, 0.5 mmol, 1 equiv) and HBPin (36 μL, 0.25 mmol, 0.5 equiv) were then placed in the J. Young NMR tube via syringe. The J. Young NMR tube was capped and heated in the NMR probe at 100 °C. The reaction was monitored by ^{1}H and ^{31}P{^{1}H} NMR spectroscopy every 20 min for conversion of starting material as well as catalyst intermediates for 4 h, after which the NMR yield of 4,4,5,5-tetramethyl-2-(5-methylthiophen-2-yl)-1,3,2-dioxaborolane showed full conversion on the basis of the limiting reagent (HBpin). See Figures S3 and S4a−d in the Supporting Information for details.

Early-Stage Kinetics of Catalytic Borylation of 2-Methylthiophene with Compound 5a, using 0.5 equiv of HBPin. Compound **5a** (20.8 mg, 0.025 mmol, 0.05 equiv) was weighed in a test tube and then transferred to a J. Young NMR tube after dissolution in cyclohexane-d_{12} (150 μL × 4). 2-Methylthiophene (49 μL, 0.5 mmol, 1 equiv) and HBpin (36 μL, 0.25 mmol 0.5 equiv) were placed in the J. Young NMR tube via syringe. The J. Young NMR tube was capped and brought out of the glovebox. Initial ^{1}H and ^{31}P NMR spectra were recorded at room temperature, and then the tube was heated in an oil bath at 100 °C. The reaction was stopped every 5 min in order to record ^{1}H and ^{31}P{^{1}H} NMR spectra at room temperature. The reaction was monitored by ^{1}H and ^{31}P{^{1}H} NMR for 20 min. See Figure S5 in the Supporting Information for details.

Catalytic Borylation of 2-Methylthiophene with Compound 5a, using 1 equiv of HBpin. Compound **5a** (20.8 mg, 0.025 mmol, 0.05 equiv) was weighed in a test tube and then transferred to a J. Young NMR tube after dissolution in cyclohexane-d_{12} (150 μL × 4). 2-Methylthiophene (49 μL, 0.5 mmol, 1.0 equiv) and HBpin (72 μL, 0.5 mmol, 1.0 equiv) were placed in the J. Young NMR tube via syringe. The J. Young NMR tube was capped and heated in the NMR probe at 100 °C. The reaction was monitored by ^{1}H and ^{31}P{^{1}H} NMR spectroscopy every 20 min for conversion of starting material as well as catalyst intermediates for 4 h, after which the NMR yield of 4,4,5,5-tetramethyl-2-(5-methylthiophen-2-yl)-1,3,2-dioxaborolane showed about 50% conversion on the basis of the substrate. See Figure S6 in the Supporting Information for details.

Generation of (dippe)Ir(H)$_2$(Bpin)$_3$ (7). A toluene-d_8 solution (0.6 mL) of compound **5a** (20.8 mg, 0.025 mmol, 1 equiv) was placed in a J. Young NMR tube. The tube was connected to a Schlenk line and then subjected to three freeze−pump−thaw cycles. The tube was opened to an atmosphere of H$_2$ gas, closed, and then placed in a precooled NMR probe at −45 °C. ^{31}P{^{1}H} and ^{1}H NMR spectroscopy showed a major resonance (∼70%) corresponding to compound **7** at 53.56 ppm and a minor resonance corresponding to compound **8** (∼30%) at 61.22 ppm.

^{1}H NMR (toluene-d_8, 500 MHz): δ 2.15 (septet, 4 H, J = 7.2 Hz) 1.33 (s, 36 H), 1.21 (dd, J = 15.5, 7.10 Hz, 12 H), 1.02 (m, 4 H), 0.95 (dd, J = 13.02, 7.1 Hz, 12 H), −11.01 (t, J = 11.4 Hz, 2 H, 9.5 Hz fwhm). ^{11}B NMR (toluene-d_8, 160 MHz): δ 38.8. ^{31}P NMR (toluene-d_8, 202 MHz): δ 53.56.

The probe was then cooled to −60 °C, and a ^{31}P NMR spectrum was recorded. With selective decoupling of the aliphatic protons, the hydride coupling was preserved and the resulting triplet proved that two hydrides are bound to iridium in compound **7**. See the Figures S7a and 8 in the Supporting Information for details.

Generation of (dippe)Ir(H)$_3$(Bpin)$_2$ (8). The J. Young tube from the previous experiment which contained **7** (∼70%) and **8** (∼30%) was warmed to −15 °C; while the relative ratio of **8** to **7** increased, the rate of conversion was slow. Therefore, the NMR tube was removed from the probe, shaken for 10 s, and placed back in the −15 °C probe. ^{31}P{^{1}H}, ^{1}H, and ^{11}B NMR showed compound **8** as the sole product (2% impurity from compound **9** was observed). See Figure S8 in the Supporting Information for details.

^{1}H NMR (toluene-d_8, 500 MHz): δ 1.96 (septet, 4 H, J = 7.2 Hz) 1.28 (s, 24 H), 1.11 (dd, J = 15.9, 7.1 Hz, 12 H), 1.02 (m, 4 H), 0.97 (s, 12 H), 0.89 (dd, J = 13.0, 7.1 Hz, 12 H), −11.21 (t, J = 5.5 Hz, 3 H).; ^{11}B NMR (toluene-d_8, 160 MHz): δ 37.4. ^{31}P{^{1}H} NMR (toluene-d_8, 202 MHz): δ 61.22.

Single crystals of compound **8** were initially isolated from a pentane solution containing compounds **5a**, **6**, and a 10-fold excess of HBPin.

The reaction solution was placed in a−35 °C freezer to crystallize. After 1 week the crystals were analyzed and found to be compound **8**.

Generation of (dippe)Ir(H)$_4$(Bpin) (9). The J. Young NMR tube containing compound **8** (from the previous experiment) was warmed to room temperature, and ^{31}P{^{1}H} and ^{1}H NMR spectra were recorded. A new signal appeared at 66.75 ppm in ^{31}P NMR (compound **9**); the ratio of compound **9** to compound **8** increased gradually. To facilitate the process, the NMR tube was taken out of the NMR probe and shaken for 15 min at room temperature. ^{31}P NMR, ^{1}H NMR, and ^{11}B NMR confirmed formation of compound **9** in 97% purity (traces of compound **8** were present). See Figures S7b and S8 in the Supporting Information for details.

^{1}H NMR (toluene-d_8, 500 MHz): δ 1.73 (m, 4 H, J = 7.1 Hz) 1.15 (m, 4 H), 1.02 (dd, J = 15.3, 7.1 Hz, 12 H), 0.92 (dd, J = 13.7, 7.1 Hz, 12 H), −11.59 (t, J = 17.0 Hz, 4 H). ^{11}B NMR (toluene-d_8, 160 MHz): δ 37.5. ^{31}P{^{1}H} NMR (toluene-d_8, 202 MHz): δ 66.75.

When the ^{31}P NMR spectrum was recorded with selective decoupling of the aliphatic protons, the hydride coupling was preserved and the resulting quintet proved that four hydrides are bound to iridium in compound **9**; see Figure S7b in the Supporting Information for details.

Single crystals of compound **9** were initially isolated from a pentane solution containing compounds **5a**, **6**, **8**, and a 10-fold excess of HBPin. The reaction mixture was placed in a−30 °C freezer to crystallize. After 2 weeks the crystals were analyzed and found to be **9**.

Synthesis of [(dippe)Ir(H)$_2$(μ-H)]$_2$ (10). A 3.0 equiv amount of MeOH (0.075 mmol, 3.1 μL) was injected in an NMR tube containing compound **9** via a syringe and ^{31}P NMR and ^{1}H NMR spectra were recorded. A new broad signal started to appear in ^{31}P NMR (compound **10**). After 12 h, ^{31}P{^{1}H} and ^{1}H NMR spectra showed a complex mixture containing ∼90% of the desired compound. The NMR tube was taken into the nitrogen-filled glovebox, and the solvent was removed under reduced pressure. The solid residue was then washed with pentane followed by recrystallization from a mixture of toluene and pentane at −35 °C to give compound **10** in 48% isolated yield (5.6 mg). The crystalline solid was dissolved in toluene-d_8, and VT NMR was obtained See Figure S9 in the Supporting Information for details.

Room-temperature ^{1}H NMR (toluene-d_8, 500 MHz): δ 0.50−3.50 (broad features, 68 H), −3.64 (br, 2 H), −12.86 (br, 2 H), −22.56 (br, 2 H). ^{31}P{^{1}H} NMR (toluene-d_8, 202 MHz): δ 77.25 (br), 75.87(br).

When the J. Young NMR tube was heated to 85 °C, a new peak appeared at δ 88.28 in the ^{31}P{^{1}H} NMR spectrum, and after 30 min at 100 °C, compound **10** was fully converted to new species.

Room-temperature ^{1}H NMR (toluene-d_8, 500 MHz): δ 0.7−1.9 (broad features for the phosphine backbone and isopropyl methyl protons), −6.80 (dd, J = 101.4, 10.5 Hz 2 H), −12.33 (br, 1H), and −13.01 (br, 2 H). ^{31}P{^{1}H} NMR (toluene-d_8, 202 MHz): δ 87.91. For VT NMR data, see Figure S10 in the Supporting Information.

■ ASSOCIATED CONTENT

Ⓢ Supporting Information

The Supporting Information is available free of charge on the ACS Publications website at DOI: 10.1021/acs.organomet.5b00525.

> Crystallographic data for **6** (CIF)
> Crystallographic data for **8** (CIF)
> Crystallographic data for **9** (CIF)
> Crystallographic data for **10** (CIF)
> NMR spectra, crystal data, and details of calculated structures (PDF)
> Coordinates from quantum chemical calculations (XYZ)

■ AUTHOR INFORMATION

Corresponding Authors
*E-mail for R.E.M.: maleczka@chemistry.msu.edu.
*E-mail for M.R.S.: smithmil@msu.edu.

Notes

The authors declare no competing financial interest.

■ ACKNOWLEDGMENTS

■ DEDICATION

We dedicate this work to the memory of Greg Hillhouse: mentor, friend, and master chemist, whose spirit lives on in the lives that he touched.

■ REFERENCES

(1) Mkhalid, I. A. I.; Barnard, J. H.; Marder, T. B.; Murphy, J. M.; Hartwig, J. F. *Chem. Rev.* **2010**, *110*, 890−931.

(2) Obligacion, J. V.; Semproni, S. P.; Chirik, P. J. *J. Am. Chem. Soc.* **2014**, *136*, 4133−4136.

(3) Schaefer, B. A.; Margulieux, G. W.; Small, B. L.; Chirik, P. J. *Organometallics* **2015**, *34*, 1307−1320.

(4) Mazzacano, T. J.; Mankad, N. P. *J. Am. Chem. Soc.* **2013**, *135*, 17258−17261.

(5) Parmelee, S. R.; Mazzacano, T. J.; Zhu, Y.; Mankad, N. P.; Keith, J. A. *ACS Catal.* **2015**, *5*, 3689−3699.

(6) Hatanaka, T.; Ohki, Y.; Tatsumi, K. *Chem. - Asian J.* **2010**, *5*, 1657−1666.

(7) Dombray, T.; Werncke, C. G.; Jiang, S.; Grellier, M.; Vendier, L.; Bontemps, S.; Sortais, J.-B.; Sabo-Etienne, S.; Darcel, C. *J. Am. Chem. Soc.* **2015**, *137*, 4062−4065.

(8) Furukawa, T.; Tobisu, M.; Chatani, N. *Chem. Commun.* **2015**, *51*, 6508−6511.

(9) Boller, T. M.; Murphy, J. M.; Hapke, M.; Ishiyama, T.; Miyaura, N.; Hartwig, J. F. *J. Am. Chem. Soc.* **2005**, *127*, 14263−14278.

(10) Cho, J. Y.; Tse, M. K.; Holmes, D.; Maleczka, R. E., Jr.; Smith, M. R., III *Science* **2002**, *295*, 305−308.

(11) Green, A. G.; Liu, P.; Merlic, C. A.; Houk, K. N. *J. Am. Chem. Soc.* **2014**, *136*, 4575−4583.

(12) Tamura, H.; Yamazaki, H.; Sato, H.; Sakaki, S. *J. Am. Chem. Soc.* **2003**, *125*, 16114−16126.

(13) Vanchura, B. A., II; Preshlock, S. M.; Roosen, P. C.; Kallepalli, V. A.; Staples, R. J.; Maleczka, R. E., Jr.; Singleton, D. A.; Smith, M. R., III *Chem. Commun.* **2010**, *46*, 7724−7726.

(14) Maleczka, R. E., Jr.; Singleton, D. A.; Smith, M. R., III Manuscript in preparation.

(15) Iluc, V. M.; Miller, A. J. M.; Anderson, J. S.; Monreal, M. J.; Mehn, M. P.; Hillhouse, G. L. *J. Am. Chem. Soc.* **2011**, *133*, 13055−13063.

(16) Mindiola, D. J.; Hillhouse, G. L. *J. Am. Chem. Soc.* **2001**, *123*, 4623−4624.

(17) Chotana, G. A.; Vanchura, B. A., II; Tse, M. K.; Staples, R. J.; Maleczka, R. E., Jr.; Smith, M. R., III *Chem. Commun.* **2009**, 5731−5733.

(18) Liskey, C. W.; Wei, C. S.; Pahls, D. R.; Hartwig, J. F. *Chem. Commun.* **2009**, 5603−5605.

(19) 18-electron complexes with the formula $(PR_3)_3Ir(boryl)_3$ are obtained when mono-phosphines are added to $(\eta^6$-arene)Ir(boryl)$_3$ complexes: Nguyen, P.; Blom, H. P.; Westcott, S. A.; Taylor, N. J.; Marder, T. B. *J. Am. Chem. Soc.* **1993**, *115*, 9329−9330.

(20) Braunschweig, H.; Dewhurst, R. D.; Gessner, V. H. *Chem. Soc. Rev.* **2013**, *42*, 3197−3208.

(21) Hebden, T. J.; Denney, M. C.; Pons, V.; Piccoli, P. M. B.; Koetzle, T. F.; Schultz, A. J.; Kaminsky, W.; Goldberg, K. I.; Heinekey, D. M. *J. Am. Chem. Soc.* **2008**, *130*, 10812−10820.

(22) Braunschweig, H.; Shang, R. *Inorg. Chem.* **2015**, *54*, 3099−3106.

(23) Alcaraz, G.; Helmstedt, U.; Clot, E.; Vendier, L.; Sabo-Etienne, S. *J. Am. Chem. Soc.* **2008**, *130*, 12878−12879.

(24) Thompson, M. E.; Baxter, S. M.; Bulls, A. R.; Burger, B. J.; Nolan, M. C.; Santarsiero, B. D.; Schaefer, W. P.; Bercaw, J. E. *J. Am. Chem. Soc.* **1987**, *109*, 203−219.

(25) Watson, P. L. *J. Am. Chem. Soc.* **1983**, *105*, 6491−6493.

(26) For a 16-electron, trigonal-bipyramidal boryl complex, see: Lam, W. H.; Shimada, S.; Batsanov, A. S.; Lin, Z.; Marder, T. B.; Cowan, J. A.; Howard, J. A. K.; Mason, S. A.; McIntyre, G. J. *Organometallics* **2003**, *22*, 4557−4568.

(27) Halpern, J. *Science* **1982**, *217*, 401−407.

(28) Other structures, such as η^2-borohydride complexes, exhibit dynamic behavior that could similarly account for exchange: Esteruelas, M. A.; López, A. M.; Mora, M.; Oñate, E. *Organometallics* **2015**, *34*, 941−946.

(29) Schnabel, R. C.; Carroll, P. S.; Roddick, D. M. *Organometallics* **1996**, *15*, 655−662.

(30) Saito, Y.; Segawa, Y.; Itami, K. *J. Am. Chem. Soc.* **2015**, *137*, 5193−5198.

(31) Ghaffari, B.; Preshlock, S. M.; Plattner, D. L.; Staples, R. J.; Maligres, P. E.; Krska, S. W.; Maleczka, R. E., Jr.; Smith, M. R., III *J. Am. Chem. Soc.* **2014**, *136*, 14345−14348.

(32) Frisch, M. J.; Trucks, G. W.; Schlegel, H. B.; Scuseria, G. E.; Robb, M. A.; Cheeseman, J. R.; Scalmani, G.; Barone, V.; Mennucci, B.; Petersson, G. A.; Nakatsuji, H.; Caricato, M.; Li, X.; Hratchian, H. P.; Izmaylov, A. F.; Bloino, J.; Zheng, G.; Sonnenberg, J. L.; Hada, M.; Ehara, M.; Toyota, K.; Fukuda, R.; Hasegawa, J.; Ishida, M.; Nakajima, T.; Honda, Y.; Kitao, O.; Nakai, H.; Vreven, T.; Montgomery, J. A., Jr.; Peralta, J. E.; Ogliaro, F.; Bearpark, M. J.; Heyd, J.; Brothers, E. N.; Kudin, K. N.; Staroverov, V. N.; Kobayashi, R.; Normand, J.; Raghavachari, K.; Rendell, A. P.; Burant, J. C.; Iyengar, S. S.; Tomasi, J.; Cossi, M.; Rega, N.; Millam, N. J.; Klene, M.; Knox, J. E.; Cross, J. B.; Bakken, V.; Adamo, C.; Jaramillo, J.; Gomperts, R.; Stratmann, R. E.; Yazyev, O.; Austin, A. J.; Cammi, R.; Pomelli, C.; Ochterski, J. W.; Martin, R. L.; Morokuma, K.; Zakrzewski, V. G.; Voth, G. A.; Salvador, P.; Dannenberg, J. J.; Dapprich, S.; Daniels, A. D.; Farkas, Ö.; Foresman, J. B.; Ortiz, J. V.; Cioslowski, J.; Fox, D. J. *Gaussian 09, Revision D.01*; Gaussian, Inc., Wallingford, CT, USA, 2009.

(33) Zhao, Y.; Truhlar, D. *Theor. Chem. Acc.* **2008**, *120*, 215−241.